



Ethanol-Based Transesterification of Rapeseed Oil with CaO Catalyst: Process Optimization and Validation Using Microalgal Lipids

Gabriela F. Ferreira^{1,2} · Luisa F. Ríos Pinto¹ · Rubens Maciel Filho¹ · Leonardo V. Fregolente¹ · James Hayward² · Jonathan K. Bartley²

Received: 18 November 2024 / Accepted: 24 December 2024
© The Author(s) 2024

Abstract

Microalgal oil has been increasingly studied as a feedstock for biodiesel production through transesterification reactions using heterogeneous catalysts. This route offers several benefits, including catalyst reuse, ease of separation, and improved safety, while addressing environmental and technical issues associated with using homogeneous acids and bases. Most studies use methanol for the transesterification, and few studies have investigated the transesterification of microalgal oil using ethanol. Beyond the environmental benefits of microalgae compared to plant-based biomass, replacing methanol with bioethanol is advantageous due to its lower cost and reduced toxicity. If the emulsion issue between the produced biodiesel and ethanol is resolved, ethanol could be a more environmentally friendly alternative for green fuel production. This study evaluated various metal oxides as catalysts for the transesterification of rapeseed oil using ethanol as both reagent and solvent to improve miscibility. From catalyst screening, CaO showed the highest fatty acid ethyl esters yield and this catalyst was then tested at different reaction times in two systems (round-bottom flask and autoclave reactor) for the transesterification of both rapeseed and microalgal (*Scenedesmus* sp.) oil. The highest reaction yield was 86.0% for rapeseed oil and 81.3% for microalgal oil using 114:1 ethanol: oil molar ratio with CaO in an autoclave reactor. This work addresses the limited studies on ethanol in microalgal oil transesterification, demonstrating the effectiveness of CaO as a catalyst. It highlights the potential of ethanol as a greener, cost-effective alternative to methanol for biodiesel production.

Highlights

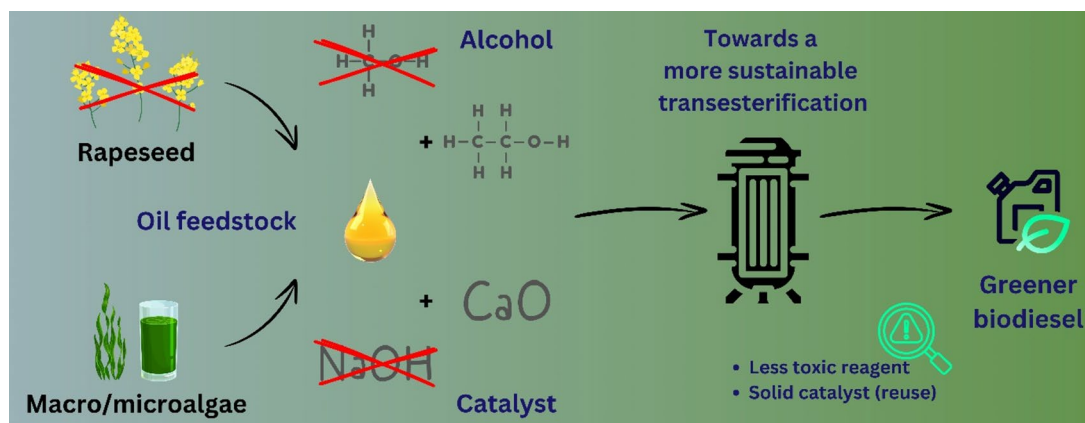
- Microalgal oil for biodiesel: greener, cost-effective with CaO catalyst.
- Ethanol reduces toxicity and cost, promising for biodiesel production.
- CaO achieves high yield in rapeseed and microalgal oil transesterification.
- Ethanol transesterification of microalgae addresses environmental issues.
- Emulsion resolved technically; further environmental and economic analysis needed.

✉ Gabriela F. Ferreira
FerreiraGabrielaF@outlook.com

¹ School of Chemical Engineering, University of Campinas
Campinas, Campinas, Brazil

² Cardiff Catalysis Institute, School of Chemistry, Cardiff
University, Cardiff, UK

Graphical Abstract



Keywords Microalgae · Lipids · Transesterification · Ethanol · Metal Oxides

Abbreviations

ANOVA	Analysis of variance
DAD	Diode-array detection
DAG	Diglyceride
DoE	Design of experiments
FAEE	Fatty acid ethyl ester
FID	Flame ionization detector
GC	Gas chromatograph
HPLC	High-performance liquid chromatography
ICDD	International Centre for Diffraction Data
ICP-OES	Inductively coupled plasma optical emission spectrometry
MAG	Monoglyceride
TAG	Triglyceride
TCD	Thermal conductivity detector
TGA	Thermogravimetric analysis

1 Introduction

Biodiesel production from renewable oils has emerged as a significant and established renewable process for replacing fossil fuel derived diesel with a non-toxic and biodegradable alternative. Among the diverse biomass sources explored, food crops (e.g., rapeseed, corn, soybean, and palm oils), non-conventional plants (e.g., *Jatropha*) [1], macro- and microalgae species [2], and waste oils [3, 4] have gained attention. Key criteria for biomass selection include productivity, oil and biodiesel yields, socioeconomic impacts, and environmental benefits. Traditional biodiesel synthesis often employs methanol with homogeneous aqueous base catalysts for high conversions. However, alternative methods such as enzymatic routes, heterogeneous catalysts, in-situ

transesterification with greener solvents, and supercritical fluids have also been extensively studied [1].

Solid heterogeneous catalysts are promising alternatives to homogeneous catalysts due to ease of separation and reuse, and environmental benefits, such as reducing aqueous waste and soap formation issues present with homogeneous base catalysts. However, heterogeneous acid catalysts, like zeolites and clays, have lower reaction rates [5] and further research on their synthesis, considering economic and environmental aspects, is required. On the other hand, basic metal oxides show competitive conversions [6] and can be improved by enhancing surface area and basic site concentration, and overcoming mass transfer limitations [7, 8]. They can be synthesized from cheap materials such as biomass ash [9], or natural [10] and industrial [11] wastes, and are divided into two categories; single metal and mixed metal oxides. CaO is widely used due to its low cost, minimal environmental impact, and relatively high basic strength [12].

Regarding biomass feedstock for transesterification, as large-scale terrestrial plant production has been associated with deforestation and high greenhouse gas emissions [13, 14], substitutes have been investigated. Microalgae are a promising alternative for biodiesel production, particularly with heterogeneous catalysts as several species have significant amounts of free fatty acids. Studies have been conducted employing in situ transesterification of microalgae with methanol using KOH/Al₂O₃ [15], SrO–C nanoparticles [16], or KF/CaO assisted by ultrasound and microwave radiation [17]; or ethanol with H₃PMo/Al₂O₃ [18]. Studies have also investigated transesterification of the lipid fraction from microalgae with methanol catalysed by WO₃/ZrO₂ [19], NaOH/zeolite [20], CaO–SiO₂ [21], CaO/dolomite [22], or Ca(OCH₃)₂ [23]; or with ethanol and Nb₂O₅/

SO₄ [24], among others. Furthermore, review studies elucidate the challenges of this process and their future perspectives [25–28].

In this study, various basic and acidic metal oxides were assessed as catalysts for the transesterification of rapeseed and microalgal (*Scenedesmus* sp.) oils using ethanol. Ethanol was chosen over methanol for its sustainability advantages, including reduced toxicity and renewable availability. Despite ethanol's challenges, such as emulsion formation [29], the study evaluated its effectiveness in biodiesel production. The reaction conditions were optimized with CaO, the most effective catalyst, and subsequently validated with purified microalgal oil, focusing on sustainable and practical application improvements.

This work stands apart from previous studies by being the first to use ethanol for biodiesel synthesis from *Scenedesmus* sp., a promising microalga strain for biofuel feedstock [30]. The research highlights CaO's efficacy in overcoming the unique challenges of ethanol-based transesterification while achieving high biodiesel yields. Additionally, the study contributes to the biofuels field by addressing both economic feasibility and environmental benefits, offering a scalable approach to renewable energy production [31].

2 Materials and Methods

2.1 Catalysts Synthesis

2.1.1 Basic Metal Oxide: CaO, La₂O₃ and MgO

Ca(OH)₂ was calcined in a tubular furnace under static air for 3 h at 600 °C (heating ramp 10 °C min⁻¹). To increase surface area, the obtained CaO (10 g) was rehydrated by refluxing in distilled water (50 mL) for 2 h, filtered, then dried (90 °C, 24 h) and calcined for 2 h at 600 °C (heating ramp 10 °C min⁻¹).

La(NO₃)₃ was calcined in a tubular furnace under static air for 4 h, at 800 °C (heating ramp 5 °C/min). The obtained La₂O₃ was stored in a desiccator before use.

Mg(OH)₂ or (MgCO₃)₄·Mg(OH)₂ was calcined in a tubular furnace under static air for 2 h at 600 °C (heating ramp 10 °C min⁻¹). The obtained MgO (10 g) was rehydrated by refluxing in distilled water (125 mL) for 3 h, dried (90 °C, 24 h), and calcined at again 600 °C (heating ramp 10 °C min⁻¹) [32].

2.1.2 Acidic Metal Oxide: Nb₂O₅, SiO₂, and WO₃

NbCl₅ (5 g) was dissolved in 200 mL deionized water. Immediately after addition, the yellow powder became white. After stirring for 3 h at room temperature, the white

precipitate was centrifuged (3,000 rpm) and washed four times with deionized water until the filtrate was at neutral pH. The obtained solid was dried at 90 °C for 48 h [33].

Silica gel (SiO₂) was not synthesized but instead, it was used as a commercial solid with a high surface area.

Na₂WO₄·2H₂O (1 g) was dissolved in 20 mL of water and then 20 mL of HCl (6 mol L⁻¹) was added under agitation. The precipitate was filtered, washed with water four times, dried (90 °C, 24 h), and calcined under static air (500 °C, 1 h) [34].

2.1.3 Mixed Metal Oxides: CaMgO, SrMgAl, and SrO/CaO-ZnO

CaMgO was prepared by a coprecipitation method, by adding a 2 M aqueous solution of the metal nitrates (Ca(NO₃)₂·4H₂O, Mg(NO₃)₂·6H₂O) into a basic aqueous solution containing NaOH and Na₂CO₃ with a pH of 8–9. The resulting precipitation was performed under vigorous stirring at 65 °C for 12 h. Finally, the solid was filtered and washed with deionized water. The resultant precursor was dried at 90 °C for 24 h and calcined in static air at 800 °C for 6 h [35].

Sr-MgAl was prepared by a sol-gel method, with an Mg/Sr molar ratio of 1.5:1. Firstly, 0.015 mol of Mg(NO₃)₂·6H₂O was dissolved in 12 mL of an ethanol solution containing 0.3 mL of HCl (35%v), under magnetic stirring. Then 0.004 mol of Al(NO₃)₃·9H₂O dissolved in 8 mL of ethanol was added dropwise followed by aqueous Sr(NO₃)₂ dissolved in ethanol (0.01 mol in 10 mL). The solution was adjusted to pH 10 by the addition of NH₄OH (30%v) and left under stirring for 24 h, the obtained gel was oven-dried at 100 °C and calcined at 600 °C for 2 h in static air (heating rate of 5 °C min⁻¹) [36].

SrO/CaO·ZnO was prepared by wet impregnation. CaO·ZnO in a 1:1 molar ratio was prepared according to mechanochemical treatment. A homogenous mixture of ZnO (0.81 g) and Ca(OH)₂ (0.75 g) powder was grounded in a pestle and mortar adding a few drops of acetone, then dried in an oven at 100 °C for 2 h. An aqueous solution of Sr(NO₃)₂ (2.1 g in 25 mL of water) was added into the prepared mixture (Ca(OH)₂ + ZnO), hence with a CaO:ZnO: SrO molar ratio of 1:1:1, and the mixture was stirred at 90 °C for 6 h. The obtained slurry was dried in an oven (90 °C), then calcined in a muffle furnace at 800 °C for 4 h [37].

All catalysts were crushed using a pestle and mortar and stored in a desiccator before use.

2.2 Catalyst Characterization

2.2.1 Thermogravimetric Analysis

Thermogravimetric analysis (TGA) was performed using a Perkin Elmer TGA 4000 under a nitrogen (N₂) flow of 20 mL min⁻¹. The analysis was conducted from 30 to 800 °C with a heating rate of 10 °C min⁻¹.

2.2.2 Surface Area Measurements

Surface area analysis was carried out using a Quantachrome ChemBET chemisorption analyser equipped with a thermal conductivity detector (TCD). Samples (50 mg) were degassed at 150 °C for 3 h prior to analysis using a Quantachrome FLOVAC Degasser. Nitrogen adsorption was assumed to correspond to half a monolayer coverage of oxygen for calculation purposes.

2.2.3 X-ray Powder Diffraction

X-ray powder diffraction (XRD) measurements were conducted using a PANalytical X'pert Pro diffractometer with a Ni-filtered CuK α radiation source operating at 40 kV and 40 mA. Diffraction patterns were recorded over the range of 10–80° 2 θ with a step size of 0.0168°. The obtained patterns were compared and matched against the International Centre for Diffraction Data (ICDD) database.

2.3 Transesterification Reactions

2.3.1 Low-severity Reaction Conditions

Catalyst screening for fatty acid ethyl ester (FAEE) synthesis from rapeseed oil (2 mL) was conducted using excess ethanol (11.1 mL, 180:1 alcohol: oil molar ratio) and 5 mol% metal oxide catalyst (0.09 g). Reactions were carried out in a 100 mL two-neck round bottom flask with a vertical condenser, immersed in a water bath. The catalyst was pre-mixed with ethanol and heated for 15 min before oil addition. The reaction conditions were 60 °C for 1 h under vigorous magnetic stirring.

Table 1 Levels of the independent variables in the design of experiments

Independent variables factor	Unit	Code	Coded actual levels		
			Low level (-1)	Medium level (0)	High value (+1)
Ethanol: oil molar ratio	-	EtOH: oil	48	114	180
Catalyst content	%m	%cat	3	4	5
Temperature	°C	T	45	60	75

Post-reaction, products were separated by adding 25 mL of hot water (60 °C) and 5 mL of hexane, followed by vortex mixing (15 s) and centrifugation (4300 rpm, 5 min). A design of experiments (DoE) study was performed with the best-performing catalyst to evaluate the effects of ethanol: oil ratio, temperature, and catalyst loading. Experiments included triplicates at the central point (Table 1). Data were analysed using Statistica 7 (Statsoft®), and reaction time was optimized and validated through duplicate experiments under the determined optimal conditions.

2.3.2 High-severity Reaction Conditions

Biodiesel synthesis was performed using rapeseed oil (6 mL), ethanol (21.1 mL), and CaO catalyst (0.16 g) in a high-pressure stainless-steel autoclave (Parr reactor). The reactor was sealed, purged three times with nitrogen, and heated to 150 °C at 20 bar for 30–120 min under 1,000 rpm agitation. After cooling the system to room temperature in an ice water bath, products were separated using the procedure described for low-severity reactions.

2.3.3 Product Analysis

FAEEs, monoglycerides (MAGs), diglycerides (DAGs), and triglycerides (TAGs) were quantified using an Agilent HC-C18 column (250 mm x 4.6 mm) coupled to an Agilent 1260 Infinity HPLC with diode-array detection (DAD). Mobile phases included (A) methanol (100–0% elution over 60 min) and (B) i-propanol/n-hexane (5:4 v/v, 0–100% elution over 60 min), followed by 10 min of isocratic elution. Samples (10 μ L) were injected after dilution to 3% (w/v) in i-propanol/n-hexane (5:4 v/v). Calibration was performed using methyl oleate, monoolein, diolein, and triolein standards.

Residual calcium content in biodiesel was analysed following Brazilian standard ABNT NBR 15,553 [38], using inductively coupled plasma optical emission spectrometry (ICP-OES) at the Analytical Centre, Chemistry Institute, University of Campinas.

2.3.4 Reaction Kinetics

Transesterification was modelled as a pseudo-first-order reaction due to the use of excess alcohol (ethanol), with a molar ratio far exceeding the stoichiometric requirement (3:1). The pseudo-first-order kinetics in transesterification using excess alcohol is well-supported by literature, allowing the assumption of pseudo-first-order kinetics to simplify modelling and calculations [39, 40]. Conversion of TAGs at different times was used to calculate apparent first-order rate constants (k_{app}) using Eq. (1).

$$-\ln(1 - X) = k_{app} \cdot t \quad (1)$$

where X is the oil conversion to FAEE at time t , and k_{app} is the apparent rate constant (min^{-1}).

The activation energy of the reaction was experimentally determined by conducting transesterification at varying temperatures (45, 60, and 75 °C), and applying the Arrhenius equation (Eq. 2). A plot of $\ln k_{app}$ versus $1/T$ yields a straight line, with slope providing $-E_a/R$.

$$k_{app} = A \cdot \exp(-E_a/RT) \quad (2)$$

where A is the pre-exponential factor, E_a is the activation energy (J mol^{-1}), R is the gas constant ($8.314 \text{ J mol}^{-1} \text{ K}^{-1}$), and T is the absolute temperature (K).

2.3.5 Microalgal oil

The best-performing catalyst and reaction conditions were tested with *Scenedesmus* sp. LF01 microalgal oil. Wet biomass was grown and donated by Algae Biotecnologia Ltda., with inoculum provided by the Federal University of São Carlos (UFSCar). Biomass was dried using a spray dryer (DR-0,4 AIR SPRAY PROCESS) and lipids extracted via ultrasound-assisted hexane extraction (60 °C, 1 h; solvent-to-biomass ratio 10:1 v/m). Extracted lipids were purified using silica gel and bentonite in a chromatographic column with chloroform as the mobile phase. The resulting oil was yellow, extracted from the viscous, dark green lipid fraction [41].

Under optimal conditions, the catalyst and reaction setup were evaluated for microalgal oil via ASTM D6584 [42] and EN14105, using gas chromatography with flame ionization detection (GC-FID, Agilent 7890 A).

3 Results and Discussion

3.1 Catalyst Characterization

Basic metal oxides were produced by calcination of the different precursors. TGA was conducted to evaluate the required calcination temperature for the decomposition of each catalyst precursor (Fig. 1). Generally, a higher calcination temperature will result in a more crystalline solid [43] and an intermediate temperature (e.g., between 100 and 1000 °C) will maximize surface area [32, 43, 44]. Thus, these two properties should be considered for the optimal conditions. TGA can also predict synthesis efficiency if a simple mass balance is used to calculate the mass loss required by the precursor to completely transform into the metal oxide. Based on the molecular masses, $\text{Ca}(\text{OH})_2$ would require a

mass loss of 24%, La_2O_3 of 50%, $\text{Mg}(\text{OH})_2$ of 31%, and $(\text{MgCO}_3)_4 \cdot \text{Mg}(\text{OH})_2$ of 49%. Depending on the elements present in precursors, the mass loss is due to H_2O , CO , CO_2 , and NO_x release.

From Fig. 1a, CaO formation from $\text{Ca}(\text{OH})_2$ was nearly completed around 500 °C. The additional decrease at higher temperature could be due to CO_2 poisoning that could form CaCO_3 in the precursor [45]. The $\text{La}(\text{NO}_3)_3$ decomposition in Fig. 1b showed three stages of thermal decomposition, from room temperature to 200 °C, then 480 °C, and finally, 650 °C. The first could be related to water loss and the other two to mass losses from the releasing of nitric acid, nitrogen dioxide, water, and oxygen [46]. Figure 1c showed typical curves for MgO from different precursors, but the red coloured curve had a higher mass loss than expected, which could be associated with interstitial water molecules adsorbed in pores due to the size of $(\text{MgCO}_3)_4 \cdot \text{Mg}(\text{OH})_2$. MgO is obtained at around 400 °C from $\text{Mg}(\text{OH})_2$ and around 500 °C from $(\text{MgCO}_3)_4 \cdot \text{Mg}(\text{OH})_2$. Guided by the TGA experiments (Fig. 1a and c), both CaO and MgO calcinations were performed at 600 °C. Despite showing a minor mass loss from 600 to 680 °C, the CaO catalyst calcined at 700 °C was tested and did not show an improvement in FAEEs yield, over the material calcined at 600 °C. According to Fig. 1b, La_2O_3 requires a temperature higher than 700 °C for complete decomposition of $\text{La}(\text{NO}_3)_3$, thus the temperature employed for this calcination was 800 °C.

Surface area and pore radius were calculated based on BET/BJH methodology. As previously stated, the more crystalline a solid, the lower the surface area. However, a high surface area material is desired to obtain the most active sites possible to increase reaction yield. Table 2 shows the results for all catalysts tested in this work. For both CaO and MgO catalysts, an increase in surface area was observed when the materials underwent a rehydration step between calcinations [47]. Among the basic metal oxides, rehydrated MgO showed the highest surface area, $73.3 \text{ m}^2 \text{ g}^{-1}$, with the highest pore radius also obtained for MgO, 32.1 \AA , but from a different precursor, $(\text{MgCO}_3)_4 \cdot \text{Mg}(\text{OH})_2$. Among acidic metal oxides, Nb_2O_5 showed a relatively high surface area ($65.7 \text{ m}^2 \text{ g}^{-1}$) despite not being calcined but produced from a synthesis strategy. Finally, CaMgO produced by coprecipitation reached the highest surface area, $70.7 \text{ m}^2 \text{ g}^{-1}$, which could be an advantage over the other mixed metal oxides.

According to IUPAC, adsorbents and catalysts can be classified as macroporous if pore sizes are higher than 50 nm, mesoporous between 2 and 50 nm, and microporous below 2 nm [48]. The produced metal oxides were either micro- or mesoporous. Nonetheless, no catalyst had a pore radius smaller than 1.6 nm. From a study of the hydrodynamic radius of palm oil in various solvent systems, the average

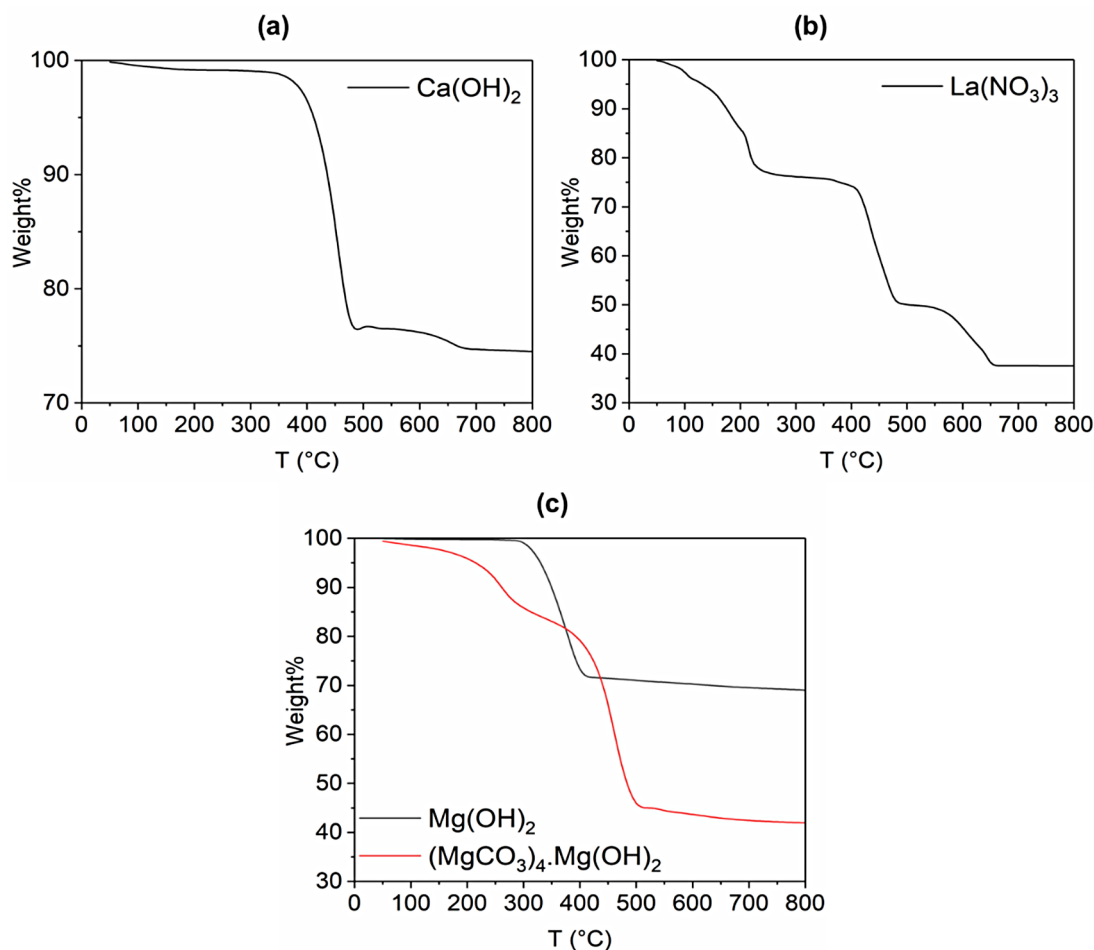


Fig. 1 TGA curves of precursors decomposition in N_2 to obtain basic metal oxides: (a) $Ca(OH)_2$, (b) $La(NO_3)_3$, and (c) $Mg(OH)_2$, and $(MgCO_3)_4 \cdot Mg(OH)_2$

Table 2 Surface area measurements for the synthesised metal oxide catalysts

Catalyst		Precursor/method	Surface area / $m^2 g^{-1}$	Pore radius / Å
Basic	CaO	$Ca(OH)_2$	13.72	16.14
		Rehydrated CaO	22.93	17.39
	La_2O_3	$La(NO_3)_3$	9.04	17.41
	MgO	$Mg(OH)_2$	33.60	18.76
		Rehydrated MgO	73.28	20.35
		$(MgCO_3)_4 \cdot Mg(OH)_2$	69.32	32.13
Acid	Nb_2O_5	$NbCl_5$	65.73	16.11
	SiO_2	-	-	-
	WO_3	$Na_2WO_4 \cdot 2H_2O$	8.10	20.33
Mixed	CaMgO	Co-precipitation	70.71	17.41
	Sr-MgAl	Sol-gel	28.08	18.79
	SrO/CaO-ZnO	Wet impregnation	4.15	26.34

value was calculated as 0.722 nm [49]. Although the fatty acid composition may influence TAG size, an overestimated value of 1 nm can be considered, thus an appropriate pore radius would be key to avoid steric impediment of large

molecules. Coupled with a high surface area to increase active sites, larger pores allow a better use of both external and internal areas of the solid materials. XRD analysis was performed to evaluate the catalysts produced and determine their crystallinity. As shown in Fig. 2, basic heterogeneous catalysts can be unstable under normal ambient conditions, being susceptible to reaction with water and CO_2 from the atmosphere. Comparing fresh CaO to the material stored for 24 h, a number of intense reflections assigned to $CaCO_3$ and $Ca(OH)_2$ were observed, while stored La_2O_3 reflections were assigned to $La(OH)_3$. Previous studies have shown that MgO catalysts also deactivate within a few hours of calcination due to water absorption. These oxides were found to be unstable, even when stored in a desiccator, and so in situ XRD analysis was conducted for CaO to evaluate this process. Figure 3 shows the XRD pattern of the $Ca(OH)_2$ precursor initially at 50 °C (a), after heating to 600 °C for 2 h to form CaO (b), after cooling the calcined catalyst to 50 °C (c), after holding the catalyst at 50 °C for 12 h (d). It was observed that a few hours after calcining and cooling

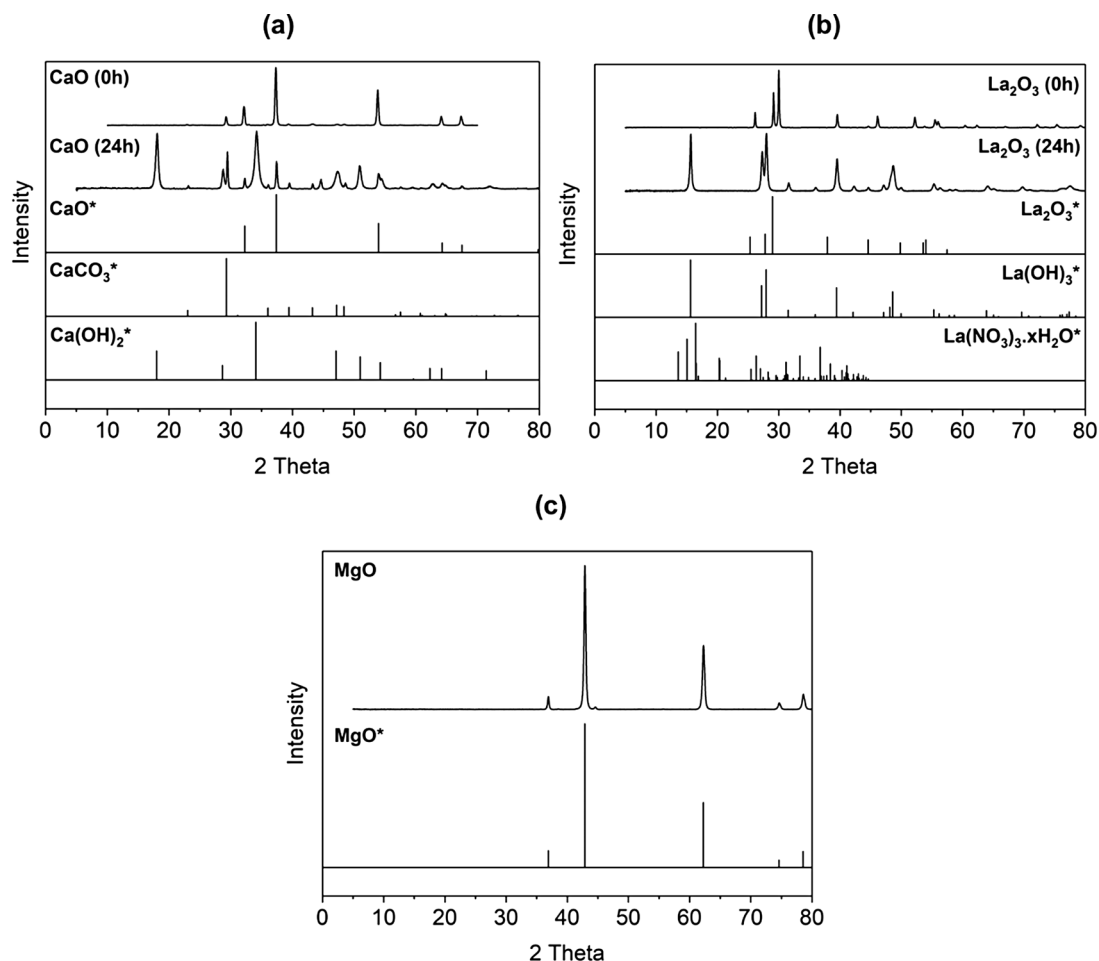


Fig. 2 XRD results for basic metal oxides synthesized and their standards (*): (a) CaO, (b) La₂O₃, and (c) MgO. Standards references: CaO (01-082-1690), CaCO₃ (01-086-2340), Ca(OH)₂ (00-001-1079),

La₂O₃ (00-024-0554), La(OH)₃ (01-083-2034), La(NO₃)₃.4H₂O (00-047-0888), and MgO (01-087-0651)

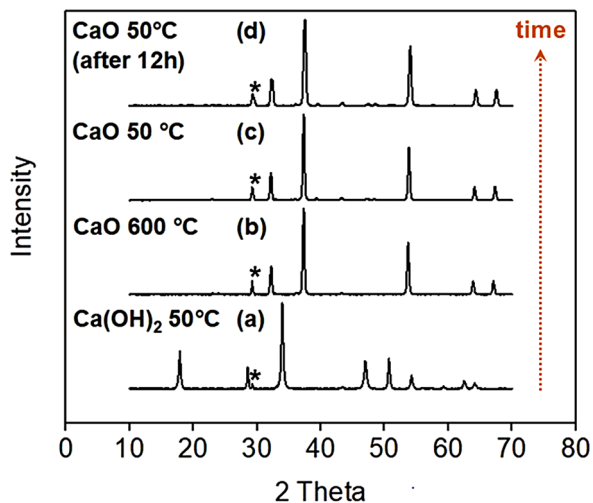


Fig. 3 XRD results evaluated during calcination of Ca(OH)₂ to produce CaO, in four steps: (a) initially at 50 °C, (b) after 2 h calcination at 600 °C, (c) after cooling to 50 °C, and (d) left for 12 h, with peaks identified from CaCO₃ (*)

down, the peak width of the reflections increased indicating this instability, despite the sample being enclosed in the in situ XRD holder with less contact with ambient air, and a new reflection at around $2\theta = 30^\circ$, appears which can be assigned to CaCO₃.

The stability problem was not observed for the acid catalysts, and the XRD patterns did not change after preparation (Fig. 4). The XRD patterns of the mixed metal oxides are shown in Fig. 5. From the identified peaks, CaMgO synthesis was confirmed by showing the presence of CaO and MgO. Sr-MgAl, on the other hand, showed varying peaks, with the presence of phases containing N and Cl from the synthesis procedure. Finally, SrO/CaO-ZnO had peaks that corresponded partially to SrZnO₂, ZnO, CaO, and SrCO₃, which indicate an efficient synthesis but possible reaction with CO₂ from the air.

All prepared catalysts were tested for transesterification reaction. To ensure the basic metal oxides had not adsorbed water or CO₂ prior to testing, these catalysts were tested

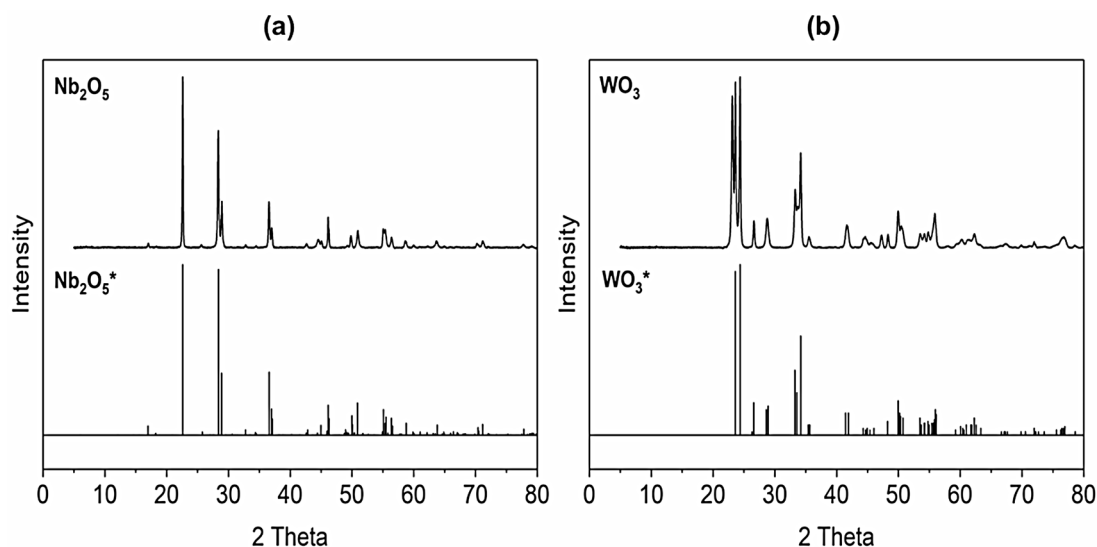


Fig. 4 XRD results for acid metal oxides synthesized and their standards (*): (a) Nb_2O_5 and (b) WO_3 . Standards references: Nb_2O_5 (01-071-0336), and WO_3 (00-024-0747)

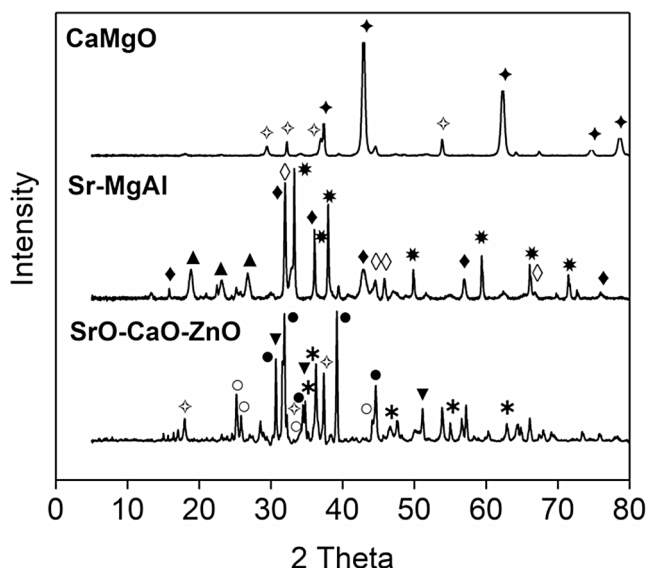


Fig. 5 XRD of mixed metal oxides: CaMgO, with peaks identified from CaO/Ca(OH)₂(◇) and MgO(★); Sr-MgAl, with peaks identified from AlN(★), Al₂O₃·3SrO(◇), Sr₃Al₂O₆(◆), and Mg(NH₄)Cl₃(H₂O)₆(▲); and SrO/CaO-ZnO, with peaks identified from SrO(▼), SrCO₃(○), SrZnO₂(●), CaO/Ca(OH)₂(◇), and ZnO(★)

immediately after calcination and were cooled in a desiccator until ambient temperature was reached.

3.2 Transesterification Reaction of Rapeseed oil

All reaction yields for transesterification (1 h) at low-severity conditions using basic or acid catalysts were less than 10%, except for CaO that achieved around 35%. Mixed metal oxides also showed a very low yield (< 1%), thus were disregarded and the CaO catalyst was selected for further

Table 3 Design of experiments (2³) for the transesterification reaction with ethanol

Run	Temperature	Catalyst	Ethanol: oil	Biodiesel (FAEE) yield / %
1	-1	-1	-1	13.5
2	-1	-1	1	15.8
3	-1	1	-1	13.5
4	-1	1	1	14.9
5	1	-1	-1	31.6
6	1	-1	1	36.0
7	1	1	-1	34.7
8	1	1	1	37.3
9	0	0	0	20.2
10	0	0	0	24.7
11	0	0	0	24.3

study. CaO-based catalysts derived from synthetic chemicals or cheap sources (e.g., residual biomass) are shown to be suitable for biodiesel synthesis [50] and are preferable due to significantly lower costs but similar reaction yield.

A design of experiments was devised to evaluate the effects of temperature, catalyst loading, and alcohol to oil ratio on the reaction yield. The Pareto-chart obtained for this two-level full factorial design with triplicates at the centre point (Table 3) is shown in Fig. 6. The use of triplicates at central points allows for an estimation of pure error, which can be used to validate the experimental results and ensure that observed effects are due to changes in the factors studied, rather than random noise or inherent variability. The statistical analysis was carried out considering a 95% confidence level ($p=0.05$). The Analysis of Variance (ANOVA) for the study is shown in Table 4, which passed both F-tests. In the first F-test, the calculated F-value was 91.36, significantly

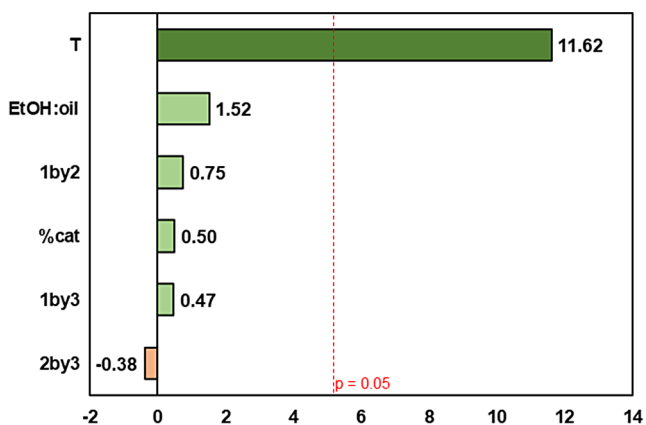


Fig. 6 Pareto chart of low-severity reaction using CaO as catalyst

Table 4 ANOVA table obtained from transesterification design of experiments ($R^2 = 0.98$)

Factor	SS ^a	DF ^b	MS ^c	F-value	p-value
T	838.45	1	838.45	135.16	0.007
%cat	1.53	1	1.53	0.25	0.669
EtOH: oil	14.31	1	14.31	2.31	0.268
T and %cat	3.51	1	3.51	0.57	0.530
T and EtOH: oil	1.36	1	1.36	0.22	0.686
%cat and EtOH: oil	0.91	1	0.91	0.15	0.738
Lack of fit	5.66	2	2.83	0.46	0.687
Pure error	12.41	2	6.20		
Total SS	878.14	10			

^aSum of Squares, ^bDegrees of Freedom, ^cMean Squares

higher than the tabulated F-value (3,7)=4.35. In the second F-test, the calculated F-value was 0.76, lower than the tabulated F-value (5,2)=19.3. According to the ANOVA table, the F-value for temperature was 135.16, which is significant at $p=0.05$, indicating that temperature has a strong effect on the reaction yield. In contrast, for other factors, such as catalyst content, the F-value was much lower, suggesting these factors do not significantly influence the yield under the tested conditions. The R^2 value of 0.98 in the ANOVA table indicates that the model explains 98% of the variance in the data, demonstrating adequate fit. The null hypothesis (H_0) assumes no significant effect of the independent variables (temperature, catalyst content, ethanol: oil ratio) on the yield of FAEs. Since the calculated F-value exceeds the tabulated F-value for temperature, we reject the null hypothesis, indicating that the variables significantly affect the reaction yield.

In the experimental range studied, the only significant variable was reaction temperature. Consequently, lower catalyst loading and ethanol: oil molar ratio could be investigated to reduce operational costs. Temperature is often a major player in biodiesel production [51], especially when using heterogeneous catalysts, which could increase costs, hence the need to optimise this reaction parameter. On the

other hand, studies have shown that alternative reaction systems such as photocatalysis using sunlight as energy source can reach high conversions while reducing costs [52].

Given that only temperature was significant, the regression model can be simplified to focus on this factor. The model is: $\text{Yield} = 24.227 + 20.475(\text{Temperature})$. Here, the intercept is 24.227, and the coefficient for temperature is 20.475, indicating a strong positive relationship between temperature and biodiesel yield. Since the other factors (catalyst and ethanol: oil ratio) were not significant, they are excluded from the model.

For the following experiments, 3 mol% of catalyst was employed, with 114:1 ethanol was chosen. Catalyst content was not significant within the range considered in this study; thus, the lowest value was selected. An intermediate value for excess ethanol was chosen because, as visually observed, this solvent/reactant volume resulted in a better miscibility with oil as well as the reaction mixture with the catalyst. As the temperature was the only significant variable at $p=0.05$ with a positive effect, the maximum value was maintained, which is close to ethanol boiling point.

The kinetics for the best conditions (75 °C, 3 mol% CaO, and 114:1 EtOH: oil) was studied to evaluate when the reaction reaches equilibrium i.e., yield is constant. From Fig. 7a, it is possible to observe that the maximum yield (around 91%) is achieved after 6 h, a time considerably longer than the necessary for the reaction at high-severity conditions (Fig. 7b), which achieved 86% yield after 90 min.

Kinetic parameters were calculated by plotting $-\ln(1-X)$ versus t for transesterification at low-severity conditions from 0 to 6 h according to the results in Fig. 7. The angular coefficient corresponded to the apparent reaction rate constant, $k_{app} = 0.0131 \text{ min}^{-1}$, with $R^2 = 0.996$. This shows that the reaction follows the (pseudo) first-order rate law, as expected when excess ethanol was used. The reported k_{app} value is consistent with literature findings for basic metal oxides, which commonly exhibit values range from 0.01 to 0.02 min^{-1} ; for instance, the transesterification of microalgae oil using CaO- Al_2O_3 catalyst achieved $k_{app} = 0.02 \text{ min}^{-1}$ under optimized conditions [26]. The differences could be due to factors such as catalyst surface area, ethanol interaction issues, or reaction mass transfer limitations.

Activation energy was estimated by obtaining new reaction curves under different temperatures as previously stated, and the following reaction points were obtained: $k_{app} = 0.0036 \text{ min}^{-1}$ at 60 °C and $k_{app} = 0.0017 \text{ min}^{-1}$ at 45 °C ($R^2=0.97$). The estimated value was $E_a = 62.4 \text{ kJ mol}^{-1}$. The reported activation energy is higher than most studies for metal oxides, which typically fall between 25 and 40 kJ mol^{-1} [26]. This discrepancy could stem from differences in experimental design, such as temperature ranges or ethanol's complex interaction with the catalyst. The higher E_a

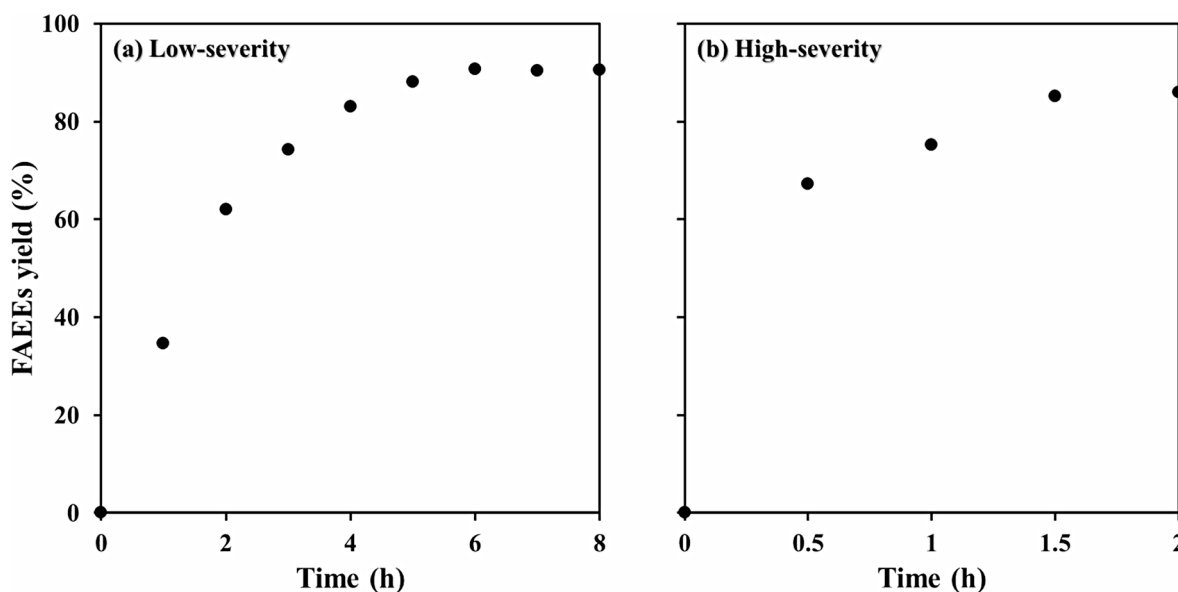


Fig. 7 Transesterification reaction of rapeseed oil using CaO (3% m) as catalyst: (a) low-severity with excess ethanol (114:1), and (b) high-severity with excess ethanol (114:1)

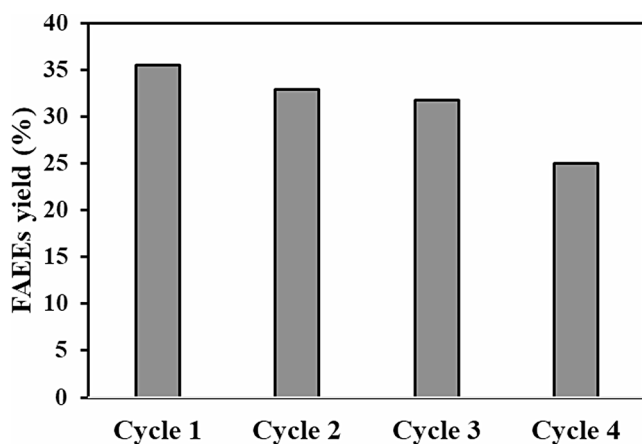


Fig. 8 Catalyst reusability of CaO in transesterification

suggests that this process is more temperature-sensitive, which may hinder scalability without further optimization. However, the study's focus on ethanol as a greener alcohol alternative and its application to microalgae oil presents significant environmental benefits.

The catalyst reusability of CaO was tested in a transesterification reaction. After 1 h of reaction, the catalyst was recovered through filtration and simple washing, then dried and calcined under the same conditions. This procedure resulted in a FAEs yield of 10.6%, compared to 35.5% with the fresh catalyst. By modifying the regeneration procedure to include a rehydration step before calcination, a similar yield to the fresh catalyst (32.9%) was achieved. Further reuse cycles are illustrated in Fig. 8. Although these results suggest a feasible method for catalyst reuse, additional research is needed. According to review studies,

CaO-based catalysts can be reused for a few cycles when a proper regeneration step is applied to minimize efficiency loss [53]. However, a significant reduction in catalytic activity was observed after the third reuse cycle in this study.

Additionally, leaching of the active phase is another challenge that might reduce the catalyst efficiency [53]. The residual Ca in biodiesel produced after 6 h under low-severity conditions was found to be 480 ± 70 ppm, which is greater than the specified limit of 5 ppm in quality standards [54]. Review studies have indicated that despite being an efficient catalyst, CaO can leach during the reaction [8]. To overcome this problem, Kouzu et al. [55] purified biodiesel by passing it through a column packed with cation-exchange resin to remove the leached CaO catalyst. They tested different process conditions and were able to achieve 100% removal of Ca (200 ppm) by adding methanol to improve mass transfer.

3.3 Validation of Microalgal oil

Microalgal oil was tested under the same conditions described in Fig. 7 for comparison. Fewer reaction times were conducted to trace these curves due to feedstock quantity limitations. Under low-severity reaction conditions (Fig. 9a), the ethyl esters yield was 70.2% after 8 h, around 20% lower than the yield of FAE from rapeseed oil. Several process parameters may have influenced this inferior result, with the microalgal oil purity the main contributing factor. Despite using an efficient purification step by simple adsorption as previously described, which increased the TAGs content, the obtained oil was not composed entirely

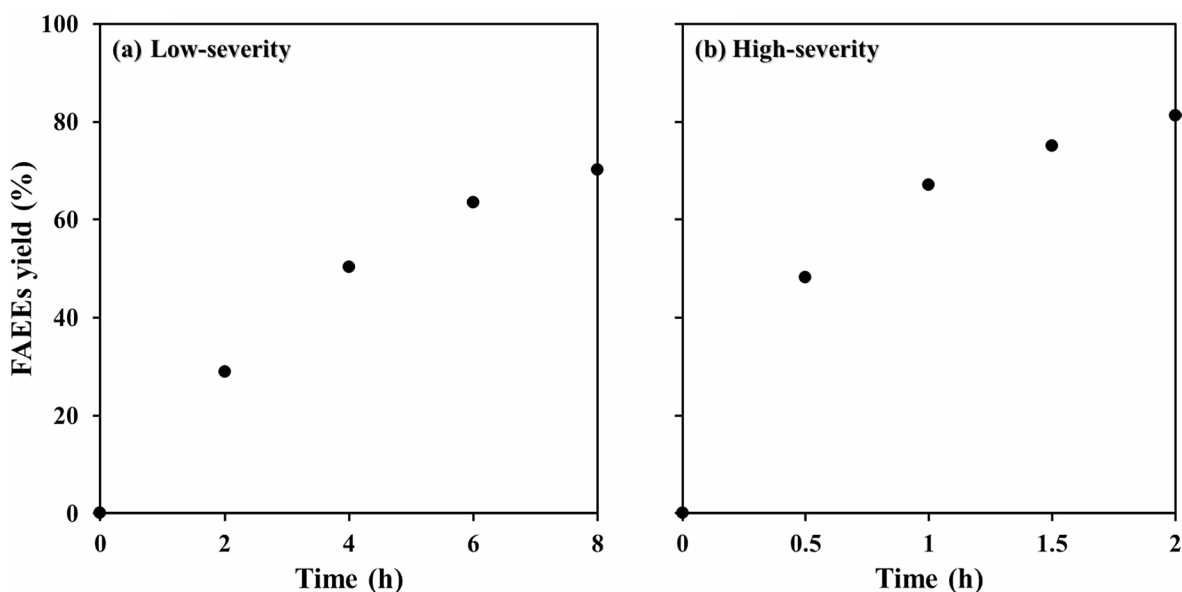


Fig. 9 Transesterification reaction of microalgal oil using CaO (3% m) as catalyst: (a) low-severity with excess ethanol (114:1), and (b) high-severity with excess ethanol (114:1)

Table 5 Literature review for the transesterification reaction of microalgal oil using ethanol and heterogeneous catalysts

Microalgae / Catalyst	System	Reaction rate	Yield	Reference
<i>Chlorella minutissima</i> ¹ H ₃ PMo/Al ₂ O ₃	Autoclave-type reactor (Parr 3830 Series, Illinois). Ethanol: oil 120:1, catalyst 20%, 200 °C, 6 h, 300 rpm	0.805	η = 96.6% - ¹ H-NMR	[18]
<i>Nannochloropsis gaditana</i> ¹ H ₃ PMo/Al ₂ O ₃	Autoclave-type reactor (Parr 3830 Series, Illinois). Ethanol: oil 120:1, catalyst 20%, 200 °C, 6 h, 300 rpm	0.808	η = 96.9% - ¹ H-NMR	[18]
<i>Nannochloropsis oculata</i> CaO/Al ₂ O ₃	Batch reactor. Ethanol: oil 48:1, catalyst 12%, 50 °C, 2 h	4.125	η = 99.0% -GC-FID	[56]
<i>Prototheca moriformis</i> Metallo-stannosilicate	Open glass reactor (100 mL) equipped with a reflux condenser and a magnetic stirrer, immersed in a thermostatic bath. Ethanol: oil 30:1, catalyst 3%, 100 °C, 12 h, 900 rpm	2.683	η = 96.6% -GC-FID	[57]
<i>Scenedesmus</i> sp. CaO	Round bottom flask (100 mL) equipped with a condenser and magnetic stirrer in a thermostatic bath. Ethanol: oil 114:1, catalyst 3%, 75 °C, 8 h, 300 rpm	2.925	η = 70.2% -GC-FID	This study
	Autoclave-type reactor (100 mL). Ethanol: oil 114:1, catalyst 3%, 150 °C, 2 h, 1,000 rpm	13.550	η = 81.3% -GC-FID	This study

¹In situ transesterification; Yield (η) in %m; Reaction rate in (g FAEE) (g catalyst)⁻¹ h⁻¹

of acylglycerols. Other minor constituents may include waxes, hydrocarbons, residual polar lipids, and free fatty acids. Consequently, commercial rapeseed oil was expected to achieve a higher yield. Nonetheless, microalgae showed a promising result for FAEE production using CaO catalyst, which had not previously been tested for transesterification with ethanol.

In Fig. 9b, the comparison of the different biomass sources was found to be more competitive under high-severity conditions, with a reaction yield from microalgal oil of 81.3% after 2 h compared to 86.0% for commercial vegetable oil. The major difference was at shorter reaction times, when

microalgae oil reached 48.2% yield after 30 min compared to 67.3% from rapeseed oil.

Table 5 shows the results of previous studies investigating microalgae transesterification with ethanol and a heterogeneous catalyst. In addition to the weaknesses of microalgal oil purification discussed, the superior reaction yields from other studies in Table 5 can be attributed to process conditions. For the studies using autoclave reactors higher ethanol: oil molar ratios, catalyst amounts, temperature, and longer reaction times were applied [18]. For studies using glass reactors, higher temperatures and longer reaction times were applied, in addition to the differences

Table 6 Comparison of key biodiesel properties for rapeseed oil and *Scenedesmus* sp. oil

Property	Rapeseed oil	Scenedesmus sp. oil
Viscosity (mm ² /s)	3.74	3.51
Calorific Value (MJ/kg)	39.49	39.3
Oxidative Stability (h)	4,059	5038
Cetane Number (CN)	1,934	1,976
Saponification Value (SV) (mg KOH/g)	2.89	2.83
Iodine Value (IV) (g I ₂ /100 g)	2.43	3.02
Degree of Unsaturation (DU)	132.60%	118.30%
Long-chain Saturation Factor (LCSF)	47.96%	36.10%
Cold Flow Plugging Point (CFPP) (°C)	134.2	96.94

in reactor configuration. When these differences are considered, our reaction results show promise with room for improvement. Considering the reaction rate as g of product per catalyst and time, we had the highest result, 13.55 g_{FAEE} g_{catalyst}⁻¹ h⁻¹, compared to 4.125 g_{FAEE} g_{catalyst}⁻¹ h⁻¹ using CaO/Al₂O₃ [56].

The study highlights the effectiveness of using CaO, a simpler and abundantly available catalyst, in the transesterification process. Notably, the autoclave-type reactor system with *Scenedesmus* sp. and CaO achieved the highest reaction rate, with a yield of 81.3%. The results emphasize the potential of CaO as an efficient and cost-effective catalyst in biofuel production. Additionally, as purified lipids still had 5.2% of free fatty acids, a prior neutralization step could further improve these results.

Literature studies of transesterification reactions comparing methanol and ethanol showed that microalgae oil achieved one of the lowest differences between FAME and FAEE yield [57]. Except for sunflower oil that varied from 95.8% FAMES to 94.8% FAEEs yield, all the other vegetable oils had a higher decrease in yield using ethanol (palm, soybean, corn, and canola oils). Microalgae oil yielded 96.6% FAEEs compared to 98.2% FAMES. In this study, rapeseed (canola) oil conversion was more efficient than microalgal oil, but the microalgal oil yields could be improved further by optimizing the reaction conditions or improving purification of the lipids.

Finally, biodiesel properties were roughly estimated based on the fatty acid profiles of both rapeseed oil and microalgal described in previous studies [58]. Using biodiesel fuel properties equations described elsewhere [59], viscosity, calorific value, oxidative stability, cetane number, saponification value, iodine value, degree of saturation, long-chain saturation factor, and cold flow plugging point were estimated based on the fatty acid profile. Table 6 shows the estimated values. The calculated biodiesel properties for rapeseed oil and *Scenedesmus* sp. oil generally align with typical values found in the literature. Both oils exhibit viscosity and calorific values (around 3.7 mm²/s and 39 MJ/

kg) within the range expected for biodiesel, as outlined by standards like ASTM D6751 [60] (3.0–6.0 mm²/s and ~37–40 MJ/kg, respectively). The oxidative stability values (4,059 and 5,038 h) exceed the standard minimum of 3 h, indicating good storage stability. Cetane numbers were calculated to be unrealistically high, as values would typically range between 47 and 60 for biodiesel. The saponification and iodine values are consistent with typical biodiesel feedstocks, indicating a reasonable balance of fatty acid content. The degree of unsaturation and long-chain saturation factor suggest the oils have significant unsaturation, which could affect fuel performance, with *Scenedesmus* sp. oil having a more favourable cold flow plugging point (96.94 °C), suitable for colder climates. These results show that both oils have promising properties for biodiesel production, though further adjustments in the Cetane Number calculation method are needed to align with typical values.

3.4 Economic and Environmental Perspectives in Biodiesel Production

Using ethanol and CaO for biodiesel production presents both environmental and economic advantages compared to traditional methanol-based transesterification with homogeneous catalysts. Ethanol, which can be sustainably derived from crops like corn, sugarcane, and wheat [61], as well as agricultural residues and waste biomass including food waste [62], not only lowers the toxicity associated with methanol but also offers a renewable alternative that aligns with global decarbonization goals [63, 64]. By adopting ethanol, studies suggest the potential for reducing the global warming potential of biodiesel production processes, especially when the alcohol is sourced from waste biomass or surplus agricultural produce [54]. Furthermore, recycling ethanol during the transesterification process can significantly lower raw material costs, improving the overall economic feasibility [65]. In this study, a high ethanol-to-oil ratio of 114:1 was used to produce biodiesel, which may be economically impractical. This ratio was selected to overcome the challenges posed by the highly viscous and poorly purified microalgal oil, ensuring that mass transfer limitations were minimized. However, with the implementation of a more efficient process, the ethanol amount can be optimized to improve the economic feasibility of the process.

The calcination of CaCO₃ to produce CaO is an energy-intensive process that contributes significantly to CO₂ emissions, particularly in cement production, where around 68% of CO₂ emissions arise from this process. However, replacing homogeneous catalysts with CaO in biodiesel production enhances sustainability by reducing the need for extensive washing steps and minimizing soap formation. CaO, sourced from abundant materials such as hydrated

lime, bone waste, and shells, as well as from industrial by-products [66, 67], can be regenerated and reused, lowering operational costs and environmental waste. These environmental benefits extend to reduced water consumption and less chemical waste disposal, contributing to cleaner production systems. To further reduce greenhouse gas emissions, strategies like Carbon Capture and Storage (CCS) and process optimization are being explored. However, the adoption of heterogeneous catalysts on a large scale requires addressing challenges such as ensuring sufficient catalytic activity and optimizing reaction conditions for commercial viability [68, 69].

A recent analysis compared biodiesel processes using ethanol and CaO to those using methanol and homogeneous catalysts, demonstrating lower environmental impacts and improved process economics in the former. The key advantages included reduced energy demands for product separation and higher reusability of the solid catalysts, which offset initial costs [63]. However, scalability demands careful consideration of process optimization, particularly addressing reaction time and catalyst deactivation during prolonged usage.

4 Conclusions

The most promising catalyst for the transesterification reaction was found to be CaO, with temperature being the most significant reaction variable. High temperature and pressure significantly improved the reaction yield, thus requiring an economic evaluation of large-scale production using different systems. Despite the transesterification reaction yield of microalgal oil in this study showing a slightly inferior result compared to other studies of biodiesel production from microalgae using ethanol and different heterogeneous catalysts, a higher reaction rate was observed. Although an effective separation method was applied (adding water and hexane to the reaction mixture), the emulsion problem is resolved only technically. An environmental and economic analysis should be conducted to evaluate the viability of adding a new process step. Additionally, as CaO can be attained from cheap sources, it is a promising alternative to catalyse this reaction.

Acknowledgements The authors thank the support by the National Council for Scientific and Technological Development (CNPq), grant # 166844/2017-9, and the São Paulo Research Foundation (FAPESP), grant # 2015/20630-4. We also thank the Cardiff University Global Challenges Research Fund for the Small Project grant SP70.

Author Contributions Gabriela F. Ferreira: Conceptualization, Data curation, Formal analysis, Investigation, Methodology, Validation, Visualization, Writing – original draft. Luisa F. Ríos Pinto: Supervision, Visualization, Writing – review & editing. Rubens Maciel Filho:

Funding acquisition, Resources, Supervision. Leonardo V. Fregolente: Conceptualization, Funding acquisition, Investigation, Methodology, Project administration, Resources, Supervision, Writing – review & editing. James S. Hayward: Investigation, Methodology, Supervision, Validation. Jonathan K. Bartley: Conceptualization, Funding acquisition, Investigation, Methodology, Project administration, Resources, Supervision, Writing – review & editing.

Funding National Council for Scientific and Technological Development (CNPq), grant # 166844/2017-9. São Paulo Research Foundation (FAPESP), grant # 2015/20630-4. Global Challenges Research Fund, grant SP70.

Data Availability No datasets were generated or analysed during the current study.

Declarations

Ethics and Consent to Participate Not Applicable.

Consent for Publication Not Applicable.

Competing Interests The authors declare no competing interests.

Open Access This article is licensed under a Creative Commons Attribution 4.0 International License, which permits use, sharing, adaptation, distribution and reproduction in any medium or format, as long as you give appropriate credit to the original author(s) and the source, provide a link to the Creative Commons licence, and indicate if changes were made. The images or other third party material in this article are included in the article's Creative Commons licence, unless indicated otherwise in a credit line to the material. If material is not included in the article's Creative Commons licence and your intended use is not permitted by statutory regulation or exceeds the permitted use, you will need to obtain permission directly from the copyright holder. To view a copy of this licence, visit <http://creativecommons.org/licenses/by/4.0/>.

References

1. Lee JW (2013) *Advanced biofuels and bioproducts*. Springer, New York
2. Chen J, Li J, Dong W et al (2018) The potential of microalgae in biodiesel production. *Renew Sustain Energy Rev* 90:336–346. <https://doi.org/10.1016/j.rser.2018.03.073>
3. Aghel B, Gouran A, Nasirmanesh F (2022) Transesterification of waste cooking oil using clinoptilolite/ industrial phosphoric waste as green and environmental catalysts. *Energy* 244:123138. <https://doi.org/10.1016/j.energy.2022.123138>
4. Hadi Jume B, Parandi E, Nouri M et al (2023) Optimization of microreactor-assisted transesterification for biodiesel production using bimetal zirconium-titanium oxide doped magnetic graphene oxide heterogeneous nanocatalyst. *Chem Eng Process - Process Intensif* 191:109479. <https://doi.org/10.1016/j.cep.2023.109479>
5. Thornton G (2009) *Metal Oxide Catalysis.1+2*. Edited by S. David Jackson and Justin S. J. Hargreaves. *Angew Chem Int Ed* 48:3902–3903. <https://doi.org/10.1002/anie.200901285>
6. Nasreen S, Nafees M, Qureshi LA et al (2018) Review of Catalytic Transesterification Methods for Biodiesel Production. In: Biernat K (ed) *Biofuels - State of Development*. InTech
7. Védrine J (2017) Heterogeneous catalysis on metal oxides. *Catalysts* 7:341. <https://doi.org/10.3390/catal7110341>

8. Refaat AA (2011) Biodiesel production using solid metal oxide catalysts. *Int J Environ Sci Technol* 8:203–221. <https://doi.org/10.1007/BF03326210>
9. Kumar D, Sharma S, Srivastava N et al (2018) Advancement in the utilization of Nanocatalyst for Transesterification of triglycerides. *J Nanosci Technol* 4:374–379. <https://doi.org/10.30799/jnst.111.18040302>
10. Al-Sakkari EG, El-Sheltawy ST, Attia NK, Mostafa SR (2017) Kinetic study of soybean oil methanolysis using cement kiln dust as a heterogeneous catalyst for biodiesel production. *Appl Catal B Environ* 206:146–157. <https://doi.org/10.1016/j.apcatb.2017.01.008>
11. Aghel B, Gouran A, Shahsavari P (2022) Optimizing the Production of Biodiesel from Waste Cooking Oil utilizing Industrial Waste-Derived MgO/CaO catalysts. *Chem Eng Technol* 45:348–354. <https://doi.org/10.1002/ceat.202100562>
12. Guo F, Fang Z (2011) Biodiesel Production with Solid Catalysts. In: Stoytcheva M (ed) *Biodiesel - Feedstocks and Processing Technologies*. InTech
13. Intergovernmental Panel On Climate Change (2022) *Climate Change and Land: IPCC Special Report on Climate Change, Desertification, Land Degradation, Sustainable Land Management, Food Security, and Greenhouse Gas fluxes in Terrestrial ecosystems*, 1st edn. Cambridge University Press
14. Galford GL, Melillo JM, Kicklighter DW et al (2010) Greenhouse gas emissions from alternative futures of deforestation and agricultural management in the southern Amazon. *Proc Natl Acad Sci* 107:19649–19654. <https://doi.org/10.1073/pnas.1000780107>
15. Ma G, Hu W, Pei H et al (2015) Study of KOH/Al₂O₃ as heterogeneous catalyst for biodiesel production via *in situ* transesterification from microalgae. *Environ Technol* 36:622–627. <https://doi.org/10.1080/09593330.2014.954629>
16. Tangy A, Kumar VB, Pulidindi IN et al (2016) *In-Situ* Transesterification of *Chlorella vulusing* Using Cdton-Dot Functionalized Strontium Oxide as a Heterogeneous Catalyst under Microwave Irradiation. *Energy Fuels* 30:10602–10610. <https://doi.org/10.1021/acs.energyfuels.6b02519>
17. Ma G, Hu W, Pei H et al (2015) *In situ* heterogeneous transesterification of microalgae using combined ultrasound and microwave irradiation. *Energy Convers Manag* 90:41–46. <https://doi.org/10.1016/j.enconman.2014.10.061>
18. Zorn SMFE, Reis CER, Bento HBS et al (2020) *In situ* transesterification of Marine Microalgae Biomass via Heterogeneous Acid Catalysis. *BioEnergy Res* 13:1260–1268. <https://doi.org/10.1007/s12155-020-10151-6>
19. Guldhe A, Singh P, Ansari FA et al (2017) Biodiesel synthesis from microalgal lipids using tungstated zirconia as a heterogeneous acid catalyst and its comparison with homogeneous acid and enzyme catalysts. *Fuel* 187:180–188. <https://doi.org/10.1016/j.fuel.2016.09.053>
20. Dianursanti, Sistiafi AG, Putri DN (2018) Biodiesel synthesis from *nannochloropsis oculata* and *chlorella vulgaris* through transesterification process using NaOH/zeolite heterogeneous catalyst. *IOP Conf Ser Earth Environ Sci* 105:012053. <https://doi.org/10.1088/1755-1315/105/1/012053>
21. Manikandan S, Sakthivel L, Parthiban A et al (2024) Biodiesel Production from Euglena Sanguinea using Catalyst Support extracted from steel slag-optimization and kinetic study. *Catal Lett* 154:6049–6063. <https://doi.org/10.1007/s10562-024-04790-z>
22. Çakırca EE, Tekin N, İlgen G, N Akin O A (2019) Catalytic activity of CaO-based catalyst in transesterification of microalgae oil with methanol. *Energy Environ* 30:176–187. <https://doi.org/10.1177/0958305X18787317>
23. Taufiq-Yap YH, Teo SH (2014) Biodiesel Production via Transesterification of Nannochloropsis Oculata Microalga's oil using Calcium Methoxide as Heterogeneous Catalyst. *J Jpn Inst Energy* 93:995–999. <https://doi.org/10.3775/jie.93.995>
24. Loures CCA, Amaral MS, Da Rós PCM et al (2018) Simultaneous esterification and transesterification of microbial oil from *Chlorella minutissima* by acid catalysis route: a comparison between homogeneous and heterogeneous catalysts. *Fuel* 211:261–268. <https://doi.org/10.1016/j.fuel.2017.09.073>
25. Makareviciene V, Sendzikiene E, Gaide I (2021) Application of heterogeneous catalysis to biodiesel synthesis using microalgae oil. *Front Environ Sci Eng* 15:97. <https://doi.org/10.1007/s11783-020-1343-9>
26. Faruque MO, Razzak SA, Hossain MM (2020) Application of heterogeneous catalysts for Biodiesel Production from Microalgal Oil—A. *Rev Catalysts* 10:1025. <https://doi.org/10.3390/cata110091025>
27. Akubude VC, Nwaigwe KN, Dintwa E (2019) Production of biodiesel from microalgae via nanocatalyzed transesterification process: a review. *Mater Sci Energy Technol* 2:216–225. <https://doi.org/10.1016/j.mset.2018.12.006>
28. Galadima A, Muraza O (2014) Biodiesel production from algae by using heterogeneous catalysts: a critical review. *Energy* 78:72–83. <https://doi.org/10.1016/j.energy.2014.06.018>
29. Mendow G, Querini CA (2013) High performance purification process of methyl and ethyl esters produced by transesterification. *Chem Eng J* 228:93–101. <https://doi.org/10.1016/j.cej.2013.05.07>
30. Gour RS, Chawla A, Singh H et al (2016) Characterization and screening of native *Scenedesmus* sp. Isolates suitable for Biofuel Feedstock. *PLoS ONE* 11:e0155321. <https://doi.org/10.1371/journal.pone.0155321>
31. Olabi AG, Alami AH, Alasad S et al (2022) Emerging technologies for enhancing Microalgae Biofuel production: recent progress, barriers, and limitations. *Fermentation* 8:649. <https://doi.org/10.3390/fermentation8110649>
32. Xu C, Enache DI, Lloyd R et al (2010) Mgo Catalysed triglyceride transesterification for Biodiesel Synthesis. *Catal Lett* 138:1–7. <https://doi.org/10.1007/s10562-010-0365-5>
33. Marin ML, Hallett-Tapley GL, Impellizzeri S et al (2014) Synthesis, acid properties and catalysis by niobium oxide nanostructured materials. *Catal Sci Technol* 4:3044–3052. <https://doi.org/10.1039/C4CY00238E>
34. Nogueira HIS, Cavaleiro AMV, Rocha J et al (2004) Synthesis and characterization of tungsten trioxide powders prepared from tungstic acids. *Mater Res Bull* 39:683–693. <https://doi.org/10.1016/j.materresbull.2003.11.004>
35. Taufiq-Yap YH, Lee HV, Hussein MZ, Yunus R (2011) Calcium-based mixed oxide catalysts for methanolysis of *Jatropha curcas* oil to biodiesel. *Biomass Bioenergy* 35:827–834. <https://doi.org/10.1016/j.biombioe.2010.11.011>
36. Lima-Corrêa RAB, Castro CS, Damasceno AS, Assaf JM (2020) The enhanced activity of base metal modified MgAl mixed oxides from sol-gel hydrotalcite for ethylic transesterification. *Renew Energy* 146:1984–1990. <https://doi.org/10.1016/j.renene.2019.08.047>
37. Singh R, Kumar A, Chandra Sharma Y (2019) Biodiesel Production from Microalgal Oil using barium–calcium–zinc mixed Oxide Base Catalyst: optimization and kinetic studies. *Energy Fuels* 33:1175–1184. <https://doi.org/10.1021/acs.energyfuels.8b03461>
38. ABNT NBR 15553:2019 (2019) Biodiesel — determination of calcium, magnesium, sodium, phosphorus and potassium content by inductively coupled plasma optical emission spectrometry (ICPOES)
39. Trejo-Zárraga F, Hernández-Loyo FDJ, Chavarría-Hernández JC, Sotelo-Boyás R (2018) Kinetics of Transesterification Processes for Biodiesel Production. In: Biernat K (ed) *Biofuels - State of Development*. InTech

40. Noureddini H, Zhu D (1997) Kinetics of transesterification of soybean oil. *J Am Oil Chem Soc* 74:1457–1463. <https://doi.org/10.1007/s11746-997-0254-2>
41. Ferreira Gabriela F, Pinto Luisa R, Rubens FMF, Fregolente Leonardo V (2022) Lipid extraction from *Scenedesmus* Sp. Followed by purification using column chromatography. *Chem Eng Trans* 92:25–30. <https://doi.org/10.3303/CET2292005>
42. ASTM D6584-17 (2017) Standard Test Method for Determination of Total Monoglycerides, total diglycerides, total triglycerides, and free and total glycerin in B-100 Biodiesel Methyl Esters by Gas Chromatography, ASTM International, West Conshohocken, PA, www.astm.org. Standard Test Method for Determination of Total Monoglycerides, total diglycerides, total triglycerides, and free and total glycerin in B-100 Biodiesel Methyl Esters by Gas Chromatography. ASTM International, West Conshohocken, PA, www.astm.org
43. Oh SW, Bang HJ, Bae YC, Sun Y-K (2007) Effect of calcination temperature on morphology, crystallinity and electrochemical properties of nano-crystalline metal oxides (Co₃O₄, CuO, and NiO) prepared via ultrasonic spray pyrolysis. *J Power Sources* 173:502–509. <https://doi.org/10.1016/j.jpowsour.2007.04.087>
44. Shin HU, Ramsier RD, Chase GG (2016) Influence of calcination temperature on the surface area of submicron-sized Al₂O₃ electrospun fibers. *Appl Phys A* 122:145. <https://doi.org/10.1007/s00339-016-9690-x>
45. Mirghiasi Z, Bakhtiari F, Darezereshki E, Esmailzadeh E (2014) Preparation and characterization of CaO nanoparticles from ca(OH)₂ by direct thermal decomposition method. *J Ind Eng Chem* 20:113–117. <https://doi.org/10.1016/j.jiec.2013.04.018>
46. Guerreiro HM, Melnikov P, Arkhangelsky I, Wandekoken GA (2021) THERMAL DECOMPOSITION OF LANTHANUM NITRATE HEXAHYDRATE La(NO₃)₃·6H₂O. *Int J Dev Res* 11:43318–43321
47. Bartley JK, Xu C, Lloyd R et al (2012) Simple method to synthesize high surface area magnesium oxide and its use as a heterogeneous base catalyst. *Appl Catal B Environ* 128:31–38. <https://doi.org/10.1016/j.apcatb.2012.03.036>
48. Zdravkov BD (2007) Pore classification in the characterization of porous materials: a perspective. *Cent Eur J Chem* 11
49. Uemura Y, Sinmasami RA, Trinh TH, Onoe K (2020) Estimation of molecular size of triglyceride in a variety of solvents by using the intrinsic viscosity technique: an important index for transesterification of triglyceride in homogenous system. *IOP Conf Ser Earth Environ Sci* 460:012011. <https://doi.org/10.1088/1755-1315/460/1/012011>
50. Okolie JA, Ivan Escobar J, Umenweke G et al (2022) Continuous biodiesel production: a review of advances in catalysis, microfluidic and cavitation reactors. *Fuel* 307:121821. <https://doi.org/10.1016/j.fuel.2021.121821>
51. Mohammed AK, Alkhafaje ZA, Rashid IM (2023) Heterogeneously catalyzed transesterification reaction using waste snail shell for biodiesel production. *Heliyon* 9:e17094. <https://doi.org/10.1016/j.heliyon.2023.e17094>
52. Aghel B, Biabani A (2024) Using solar microreactors and photocatalysts to synthesize biodiesel. *Renew Energy* 220:119654. <https://doi.org/10.1016/j.renene.2023.119654>
53. Mazaheri H, Ong HC, Amini Z et al (2021) An overview of Biodiesel Production via Calcium Oxide based catalysts: current state and perspective. *Energies* 14:3950. <https://doi.org/10.3390/en14133950>
54. Moser BR (2011) Biodiesel Production, Properties, and feedstocks. In: Tomes D, Lakshmanan P, Songstad D (eds) *Biofuels*. Springer New York, New York, NY, pp 285–347
55. Kouzu M, Hidaka J (2013) Purification to remove leached CaO catalyst from biodiesel with the help of cation-exchange resin. *Fuel* 105:318–324. <https://doi.org/10.1016/j.fuel.2012.06.019>
56. Turkkul B, Deliismail O, Seker E (2020) Ethyl esters biodiesel production from *Spirulina* sp. and nannochloropsis oculata microalgal lipids over alumina-calcium oxide catalyst. *Renew Energy* 145:1014–1019. <https://doi.org/10.1016/j.renene.2019.06.093>
57. da Silva DA, Santisteban OAN, de Vasconcellos A et al (2018) Metallo-stannosilicate heterogeneous catalyst for biodiesel production using edible, non-edible and waste oils as feedstock. *J Environ Chem Eng* 6:5488–5497. <https://doi.org/10.1016/j.jece.2018.08.047>
58. Ferreira GF, Rios Pinto LF, Filho RM et al (2024) A comparison of Monoglyceride Production from Microalgal lipids and Rapeseed Oil Catalyzed by Metal Oxides. *ChemSusChem* e202400953. <https://doi.org/10.1002/cssc.202400953>
59. Mondal M, Khan AA, Halder G (2021) Estimation of biodiesel properties based on fatty acid profiles of *Chlamydomonas* sp. BTA 9032 and *Chlorella* sp. BTA 9031 obtained under mixotrophic cultivation conditions. *Biofuels* 12:1175–1181. <https://doi.org/10.1080/17597269.2019.1600453>
60. ASTM D6751-20A Specification for Biodiesel Fuel Blend Stock (B100) for Middle Distillate Fuels Book of Standards Volume: 05.03, Developed by Subcommittee: D02.E0, Pages: 11, DOI: 10.1520/D6751-20A, ICS Code: 75.160.20
61. Bušić A, Marđetko N et al (2018) University of Zagreb, Faculty of Food Technology and Biotechnology, Pierottijeva 6, 10000 Zagreb, Croatia, Bioethanol Production from Renewable Raw Materials and its Separation and Purification: a Review. *Food Technol Biotechnol* 56:. <https://doi.org/10.17113/ftb.56.03.18.5546>
62. Bibra M, Samanta D, Sharma NK et al (2022) Food Waste to Bioethanol: opportunities and challenges. *Fermentation* 9:8. <https://doi.org/10.3390/fermentation9010008>
63. Ghosh N, Patra M, Halder G (2024) Current advances and future outlook of heterogeneous catalytic transesterification towards biodiesel production from waste cooking oil. *Sustain Energy Fuels* 8:1105–1152. <https://doi.org/10.1039/D3SE01564E>
64. Yusuf BO, Oladepo SA, Ganiyu SA (2024) Efficient and sustainable Biodiesel Production via Transesterification: catalysts and operating conditions. *Catalysts* 14:581. <https://doi.org/10.3390/catal14090581>
65. Heo HY, Heo S, Lee JH (2019) Comparative Techno-Economic Analysis of Transesterification Technologies for Microalgal Biodiesel Production. *Ind Eng Chem Res* 58:18772–18779. <https://doi.org/10.1021/acs.iecr.9b03994>
66. Zul NA, Ganesan S, Hamidon TS et al (2021) A review on the utilization of calcium oxide as a base catalyst in biodiesel production. *J Environ Chem Eng* 9:105741. <https://doi.org/10.1016/j.jece.2021.105741>
67. Melo VME, Ferreira GF, Fregolente LV (2024) Sustainable catalysts for biodiesel production: the potential of CaO supported on sugarcane bagasse biochar. *Renew Sustain Energy Rev* 189:114042. <https://doi.org/10.1016/j.rser.2023.114042>
68. Hanein T, Simoni M, Woo CL et al (2021) Decarbonisation of calcium carbonate at atmospheric temperatures and pressures, with simultaneous CO₂ capture, through production of sodium carbonate. *Energy Environ Sci* 14:6595–6604. <https://doi.org/10.1039/D1EE02637B>
69. Carbone C, Ferrario D, Lanzini A et al (2022) Evaluating the Carbon Footprint of Cement Plants Integrated with the Calcium Looping CO₂ capture process. *Front Sustain* 3:809231. <https://doi.org/10.3389/frsus.2022.809231>